Tutorial

Marco A.G. Porcel*, Iñigo Artundo, J. David Domenech, Douwe Geuzebroek, Rino Sunarto and Romano Hoofman

Monolithic photonic integration for visible and short near-infrared wavelengths: technologies and platforms for bio and life science applications

https://doi.org/10.1515/aot-2017-0065
Received October 5, 2017; accepted December 4, 2017; previously published online March 24, 2018

Abstract: This tutorial aims to provide a general overview on the state-of-the-art of photonic integrated circuits (PICs) in the visible and short near-infrared (NIR) wavelength ranges, mostly focusing in silicon nitride (SiN) substrates, and a guide to the necessary steps in the design toward the fabrication of such PICs. The focus is put on bio- and life sciences, given the adequacy and, thus, a large number of applications in this field.

Keywords: biophotonics; integration; life science; photonics; sensors; silicon nitride; visible.

1 Introduction

Research on photonic integrated circuits (PICs) has lead to many technological advances in well-known areas such as telecommunications [1–4]. Moreover, within the last 24 years, the advances in manufacturing and design have demonstrated that complex optical components and systems used in bio- and life science could be integrated into PICs [5–7]. Different applications in biophotonics can benefit from these, like:

- Medical instrumentation: confocal and multiphoton imaging, DNA sequencers, optical coherence tomography, respiratory gas monitors, Raman spectroscopy, glucose monitors, flow cytometry, etc.
- Photonic lab-on-a-chip: rapid and automated analysis of small volume samples, *in vitro* and *in vivo* monitoring, implantable biofluoroimaging, digital electrowetting, drug discovery, etc.
- Optical sensors to measure chemical properties such as pH changes and trace gas, indirect biosensors via fluorescence, phosphorescence, or colorimetric measurements, and direct biosensors of metabolites, enzymes, environmental toxins, etc.

In this manner, such applications can benefit from the advantages of monolithic integration within PICs such as mechanical, thermal, and electro-optical stability, small size, and lightweight [2, 8–10]. Additionally, they can scale up in both complexities, with systems composed of hundreds of components, and decrease in cost, when large production volumes are reached.

A major feature for many of these applications is the short wavelength used, from the visible, 400–700 nm, to the lower near-infrared (NIR), 700–1100 nm. However, most PIC platforms traditionally proposed for telecom (e.g. silicon, InP) strongly absorb light at those wavelengths. Initially, most visible light PICs where targeted toward substrate platforms based on doped silica (also known as planar light circuits, PLC) due to its transparency in shorter wavelengths and the low propagation losses [11]. However, recent advances in silicon nitride (SiN)-based PICs are also achieving very low propagation losses on the same wavelength range while having more compact devices.

Although some visible light PICs have been reported in PLC [12, 13] (e.g. visible array waveguide grating (AWG) for spectroscopy [14]), the most relevant PICs in the visible (visible-PICs) are found in SiN. Among the reported visible-PICs, we find ring resonator (RR) filters [15, 16], microdisc

***Corresponding author: Marco A.G. Porcel,** VLC Photonics, Ed. 9B, D2, UPV, Camino de vera sn, 46022 Valencia, Spain, e-mail: marco.garcia@vlcphotonics.com
J. David Domenech and Iñigo Artundo: VLC Photonics, Ed. 9B, D2, UPV, Camino de vera sn, 46022 Valencia, Spain
Douwe Geuzebroek: LioniX International, Hengelosestraat 500, 7521 AN Enschede, The Netherlands
Rino Sunarto: PhoeniX Software B. V., Capitool 50, 7521 PL Enschede, The Netherlands
Romano Hoofman: IMEC, Kapeldreef 75, 3001 Heverlee, Belgium

www.degruyter.com/aot

resonators [17, 18], grating couplers [19], wavelength combiners [20], multi-mode interferometers (MMIs) [20], array waveguide gratings (AWGs) [21], such as the one shown in Figure 1, and diffraction gratings [23, 24].

In addition, optical waveguides feature a strong susceptibility to changes in the environment [25]. This permits the construction of PIC-based sensors in the complete transparency range of the guiding material [26]. Such sensors can then be tailored to a specific wavelength, or equivalently in spectroscopy a wavenumber, where λ (nm) $\equiv 10^7/\lambda$ (nm) (cm^{-1}), including the complete visible and NIR ranges [5, 6, 27–29].

Based on PICs, different sensing techniques have been demonstrated. The most reported ones are based on integrated Mach-Zehnder interferometers (MZIs), either by directly accessing one waveguide arm [5, 6, 30] or by inserting a structure such as a grating in the waveguide arm of the MZIs [31]. Another sensing strategy is based on measuring resonance changes in ring resonators and microdiscs [32, 33], and by forming nanocavities [34].

Because of their fast response, small sensing area, and accuracy, PIC-based sensors have been employed in research for chemical, biological, and medical measurements. Some of the most relevant applications of the reported measurements comprise chemical sensing of pollutants via chemical assay [35, 36], biological sensing of protein and bacterial detection, either via immunoassay or via label-free detection, and optogenetic applications such as cell stimulation [35, 37–39].

Alternatively, visible and short NIR PICs have also shown potential for many other applications, e.g. sources for metrology and spectroscopy (through Kerr frequency combs and supercontinuum generation) [40–42], visible light communications [43], and micro-projection systems [44, 45].

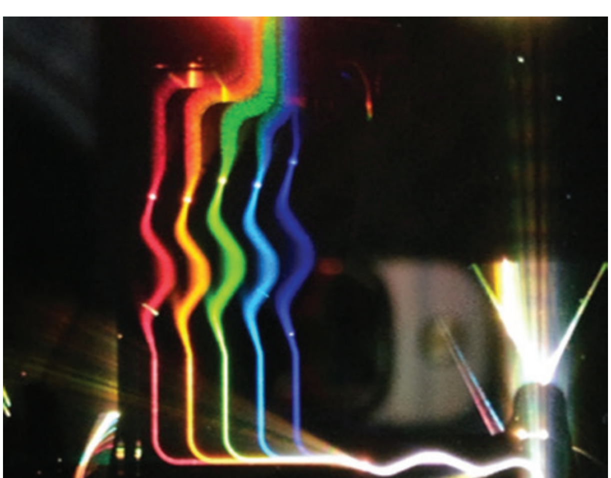

Figure 1: Visible-light spectrometer based on cascaded AWGs. Reprinted with permission of the authors [22].

In the following sections, we describe in a tutorial way the steps toward translating an optical system into a PIC, focusing on the design and fabrication options, and the trade-offs to be observed.

2 Foundry platforms for the visible

As mentioned in the introduction, due to the transparency range of the materials used for PICs, mainly two platforms are commonly used: PLC [23] and SiN. The latter offers higher confinement and, therefore, a much smaller device footprint (approximately one order of magnitude smaller). While silica has the lowest propagation and coupling losses, silicon nitride has shown, in recent years, a strong potential for low-loss visible waveguide propagation [26, 46], and many SiN-based sensors have been demonstrated [5–7, 47, 48]. Within the fabrication of SiN, a clear distinction must be made between the two main deposition techniques: low-pressure chemical vapor deposition (LPCVD) and plasma-enhanced chemical vapor deposition (PECVD). LPCVD provides high purity and reproducibility of the material deposition, requiring very high temperatures (above 700°C) [49, 50], while PECVD can be deposited at lower temperatures, which makes it compatible with metal oxide semiconductor field effect transistor (CMOS) integration [51].

The fabrication process follows standard photolithographic techniques, where a wafer is irradiated with ultraviolet light over a mask, defining this way certain areas that are later on etched chemically (dry or wet etch) to a certain depth. This process can be performed as many times as required, to define the topology of all the required structures. Additionally, other materials can be grown, and metal layers can be deposited and patterned, too, in order to implement, e.g. micro-heaters. Finally, a cladding is deposited on top, and the wafers sometimes are also planarized with benzoclyclobutene commonly known as BCB.

In Table 1, we show a summary of open-access foundries that have reported different photonic building blocks in the visible range as well as their main characteristics. TripleX is a SiN platform offered by the LioniX Int. (Enschede, the Netherlands), BioPIX is a SiN platform offered by the research instituted IMEC (Leuven, Belgium), and the last SiN platform presented is offered by CNM.

Moreover, visible PICs for bio- and life-science applications usually require different functionalities than other PIC applications, such as telecom or metrology. For example, in order to use the waveguide as a sensing

Table 1: Examples of reported devices in the respective technology platforms, where MZI stands for Mach-Zehnder interferometer, RR for ring resonator, AWG for array of waveguide grating, and MMI for multi-mode interferometer.

Foundry	LioniX	IMEC	CNM
Process	Triplex	BioPIX	–
Deposition	LPCVD	PECVD	LPCVD
Building blocks			
MZI	[52]	–	[36, 53]
RR	[16]	[47, 54]	–
AWG	[55]	[21, 54]	–
MMI	–	–	[56]
Gratings	–	[48]	[31]

device, a part of the light field such as the evanescent field needs to be guided through the elements to be sensed, e.g. gas or liquid [7]. For this purpose, the waveguides can be exposed by not having or partially removing the cladding material, etching a window over them [54], such as shown in Figure 2. For certain biologic applications, the exposed waveguide can be treated with an extra layer to functionalize the surface so that only the targeted biomolecules interact with the guided light [7, 48].

In brief, many waveguide structures can be employed for sensing [7]. Most sensors are based on changes in the propagation constant, therefore, detecting the effective refractive index of the waveguide [6, 48]. Alternatively, other sensors are based on the absorption of specific wavelengths (or spectral lines), such as for spectroscopy measurements [20, 23], or emission, such as for fluorescence [57, 58].

The fabrication process can take from 2 to 4 months, depending on the process complexity, wafer volumes, and the foundry availability. After fabrication, the back-end of the line processes is performed, such as dicing, polishing, and coating or functionalization of surfaces.

3 Photonic circuit design

The next step when developing a PIC, once the material substrate and foundry platform are selected, is to actually design and layout the circuit itself.

Complex photonic circuits are comprised of many basic waveguide structures (functional building blocks) interconnected to provide a more advanced functionality. These building blocks or circuit parts can be described as a four-port black box defined by a scattering matrix. In this manner, complex circuits can be easily modeled as a network of black box devices, providing an abstraction layer to facilitate a functional design [59].

To build complex and reliable functional circuits, the most basic building blocks have usually been predefined by each foundry in their process design kit (PDK). These PDKs include all the performance and layout information for the offered building blocks, and they are implemented for a specific design software tool [60, 61]. The degree of maturity in terms of statistic information and tolerances of the building blocks, as well as the supported software tools, depend on each foundry. The main advantage of employing a PDK relies on the ease and speed of development, saving modeling, simulation and design time, and the repeatability of the fabricated structures, reducing the uncertainty on the circuit performance and the risk of implementation errors.

In case some building blocks are not available at the PDK, they will need to be modeled, simulated, and designed to be laid out on the circuit, too. There are different software tools for that, too, providing optical mode solving and mode propagation capabilities [60–67].

Mode solvers allow to perform a 2D or 3D vectorial analysis of the mode spectrum and profiles, to do an Eigenvalue search, to track specific modes during frequency sweeps, to calculate macrobending loss and coupling efficiency, to support multiple materials and their variations, to calculate boundary conditions (periodic, symmetric, asymmetric, metallic, etc.), and to perform a frequency domain analysis (dispersion, group velocity, group index, propagation loss, effective refractive index, etc.).

When doing the mode propagation along a device, there are mainly two methods that can be used: the beam propagation method (BPM) and the finite difference in the time domain (FDTD). The BPM is best for light propagation in slowly varying non-uniform guiding structures (e.g. tapers, bends, couplers), uni-directional propagation of the total field (not mode fields), and it depends on the method to calculate the derivatives vs. the coordinates in the propagation direction. An example of a BPM simulation can be seen in Figure 3B. On the other side, the FDTD implements a discrete representation of time-dependent Maxwell's equations on a grid, and a wide bandwidth response can be extracted in a single simulation by Fourier transformation of the time-varying response of the system to some input. It is truly omni-directional, but very computational intensive, so it usually requires some optimization. Other methods include bidirectional Eigenmode propagation, Eigenmode expansion, transfer matrix, or split-step.

Once all the required building blocks are available, a complete circuit simulation can be performed [60, 61]. This mainly allows for design verification and to perform tolerance analysis over varying fabrication tolerances or design parameters. Usually, a model-based approach allows a high abstraction level, where input and output waves are modeled with intensity, phase, group delay, and chromatic dispersion parameters for both transverse electric field and transverse magnetic field polarizations. Experimental data and actual responses can be used to perform realistic simulations vs. measurements, make virtual experiments, estimate yield, extract device parameters (S-matrix), and improve the models of components. This circuit-based approach ensures efficient and high-speed computation especially for large and complex circuits, and also allows to consider system-level multiphysics, like thermal or free carrier effects.

Finally, they need to be laid out into a circuit, routing all optical and electrical connections among them and to the outside. Commercial software tools allow for hierarchical component management, flexible and parametric photonic building block definition, or semi-automatic routing. Sometimes, the circuit schematic can be used for the automatic generation of the physical layout in Graphic Databased System version 2 format for mask realization, avoiding intermediate conversions, preventing errors, and saving time. The design of the experiments is also relevant at this stage, including building block or circuit layout variations to evaluate different configurations and account for fabrication tolerances.

Depending on the requirements and the selected fabrication platform, the final circuit layout can be included in a cell either at a dedicated mask (dedicated wafer run) or using a shared mask (in a so-called multi-project wafer run) [68, 69]. The latter allows for cost-effective prototyping as the area and, thus, the costs of the masks are shared among all the end users.

The foundry collects all the cell designs coming from end users (tape-in) and performs a final design rule check (DRC) to verify that all cell layouts are compliant with the manufacturing process. All cells compose a reticle that will be replicated all over the wafer. Besides, certain features are added on the complete mask layout, like dicing lanes, alignment markers, process control monitors, etc. Once all these steps are finished, the full mask layout is ready to start fabrication (tape-out).

4 Characterization and packaging

Once the photonic circuits are fabricated, they are diced into dies, and sometimes, additional back-end processes are performed, too, such as polishing, coating, etc. While this tutorial is focusing on the design and fabrication, it is important to give a short overview of the next stages, as they will directly influence the layout.

The next step for each individual die is to be characterized from an optical perspective, to first validate the manufacturing process and, second, to evaluate the performance of the building blocks and the circuits on the die. In some cases, if vertical grating couplers are available, a preliminary die characterization can be made at wafer level, before dicing, so only known good dies are delivered to the characterization stage. The design needs to take into account all the characterization restrictions, in terms of die dimensions toward the chip holder, waveguide, and pad placement or pitch.

Because there might be design errors, foundry issues, or deviations over the fab tolerances, extensive characterization campaigns are usually required when maturing a photonic circuit, in order to validate it and have statistic measurements of every structure and parameter. This way, feedback can be provided to the design models, for iterating the complete circuit layout and achieving greater yields.

As the last step, the photonic dies will need to be usually bonded into a carrier and packaged into a housing with its corresponding electrical and optical connection ports and any other required components. For applications in the visible, this may include, e.g. collimating micro-optics, laser sources and photodetectors, microfluidic channels, or control electronics in case there are any active heaters or phase shifters included on the circuit. Once more, the layout needs to take into consideration the packaging requirements, in terms of die dimensions toward the carrier or housing, fiber port and electrical pad placement, alignment markers, etc.

There are considerable efforts to ease the packaging stage for PICs toward life science applications and lower its still high costs for volume introduction through the European pilot line PIXAPP [70].

5 Visible PIC challenges

In order to optimize PICs to guide and control visible light, it is not sufficient using a transparent material. Scattering and design errors will affect the performance more strongly due to the short wavelength of the light [25]. However, by careful design of functional circuits and mask layout, and by clean and accurate manufacturing, such losses can be minimized [26].

As a first step toward the design of a visible PIC, a designer must determine the wavelength range, or ranges, at which the final photonic circuit must function. As the wavelength is shortened, the degrading effects of

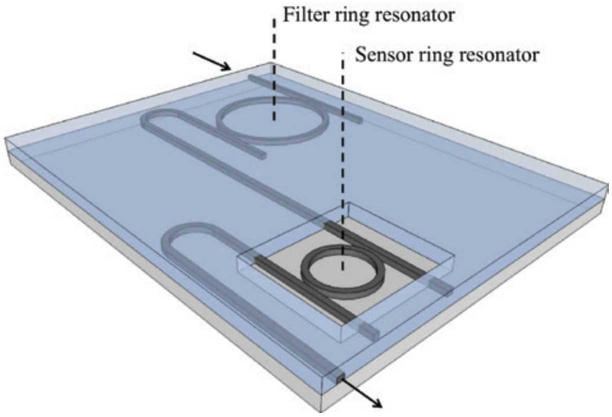

Figure 2: Example of Vernier-based ring resonator sensor (Courtesy of IMEC [71]).

material imperfections and fabrications errors, due to scattering, can become so strong that they can render the device opaque. In addition, visible applications require, in general, a much broader wavelength range to work (visible band is over 300 nm broad, compared to C-band in telecom, which is 40 nm).

An important barrier for PIC-based applications is also the scarcity of integrated light sources in SiN, although it is not always desirable such as for disposable biosensors. Most solutions are based on external lasers coupled either free space or fiber coupled to the photonic circuit [20]. Following this approach, some applications, which required multiple wavelengths at the visible spectrum, employ PIC-based light combiners [20, 72], such as shown in Figure 4. Apart from the monolithic integration process described so far, there are other more complex approaches for optical system integration using heterogeneous and hybrid techniques [73–75]. Heterogeneous integration is the process that combines multiple optical functions in a single PIC made out of two or more materials, while hybrid integration is the process that assembles one or more PICs with one or more discrete optical components into one single module. Following hybrid approaches, in the last years, great efforts have been made to add integrated sources to SiN-based PICs in the NIR, e.g. vertical-cavity surface-emitting laser (VCSELs) via adhesive bonding [75], vertical coupling to a lasing material [15, 73], or die-to-wafer bonding, mainly at NIR wavelengths. These results show the viability of such techniques to implement lasing sources and can potentially be extended toward the visible range. For certain biophotonics applications, such as photo-induced fluorescence, these integrated lasers are required to deliver very high powers, which might be challenging to achieve. However, resonating structures can be employed to rise the internal guided power [57]. Thanks to the material nature of silica and of silicon nitride, no material contribution is expected to deteriorate measurements such as the mentioned photo-induced fluorescence.

Along with the integrated light sources, integrated photo-detectors are preferable for cost effective, miniaturized devices [7]. Silicon-based platforms allow direct integration of CMOS-based photodetectors (at temperatures below 850°C) [76]. However, most SiN fabrication techniques increase the temperature above the limit for CMOS electronics [25]. Therefore, external detectors are often used, either butt-coupled to the chip facet, flip-chipped diodes over grating couplers [77], or connected via optical fibers or free space micro-optics.

Finally, as with any photonic circuit development, one of the largest challenges is on the cost of characterization, packaging, and testing, as this usually requires very high-precision (<1 μm) alignment tolerances between optical dies and fibers, or complex assemblies of microfluidics, such as shown in Figure 5, specially when targeting

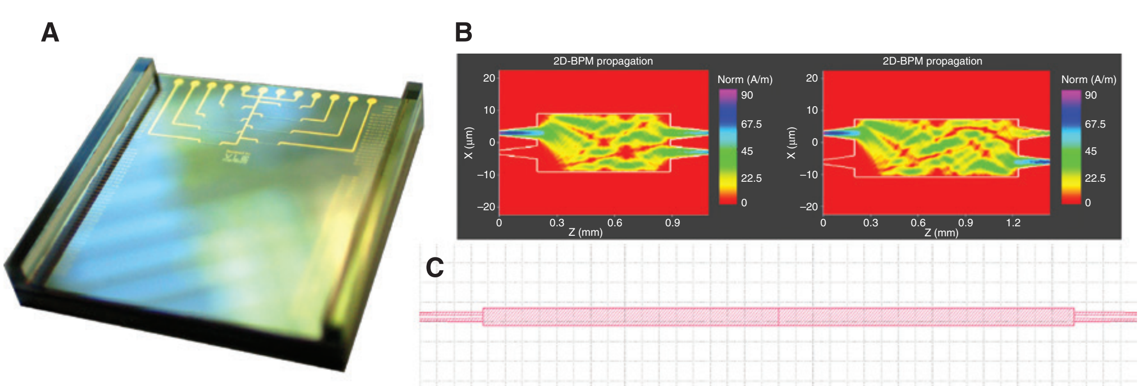

Figure 3: Example of multi-mode interferometers (MMIs) design by VLC Photonics for the TriPleX platform, (A) full device integrating many MMIs, (B) calculations for split ratios of 50/50 and 15/85 and (C) mask layout.

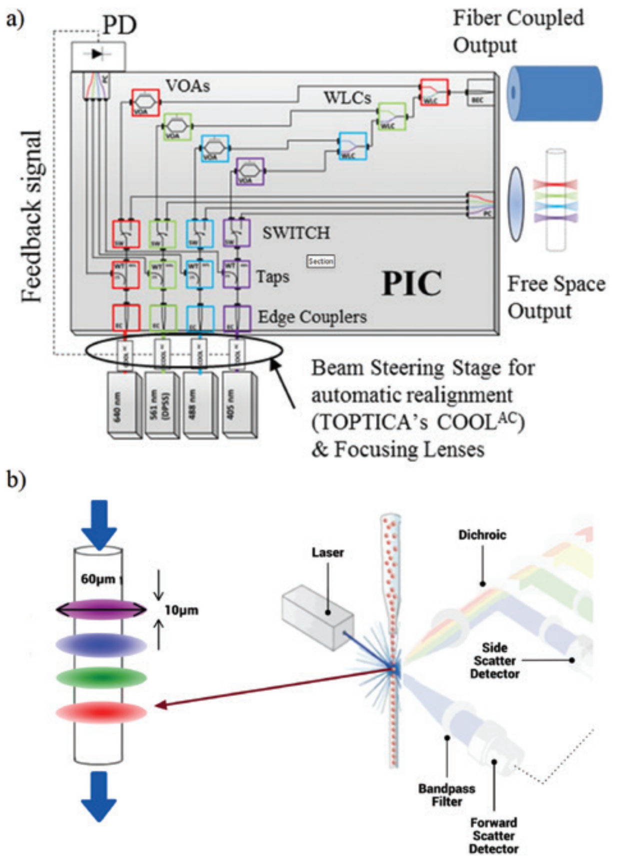

Figure 4: (A) Example of use for a wavelength combiner for a multi-color employed for time-domain resolution in flow cytometry as shown in (B) (Courtesy of the RWTH Aachen University [20]).

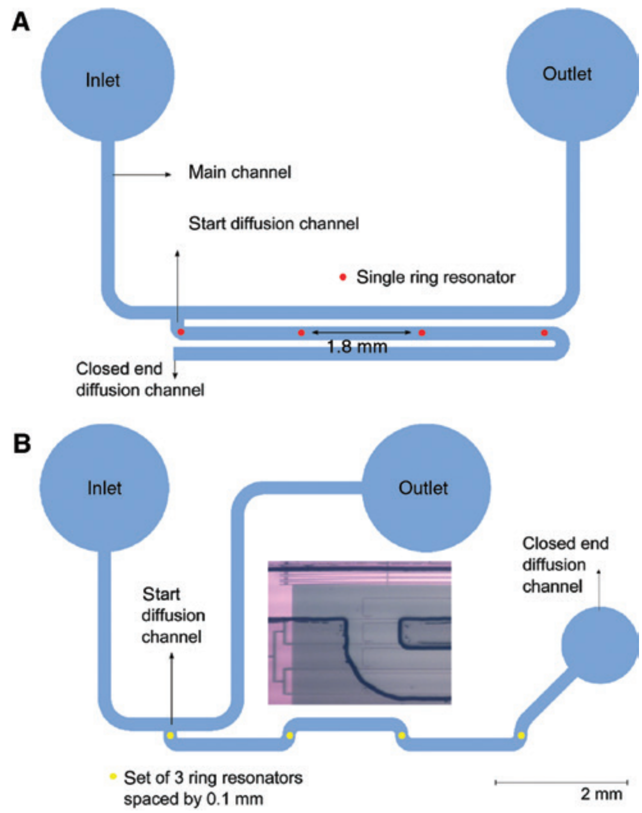

Figure 5: Example of microfluidic circuit with ring-resonator sensors for diffusion measurements. (A) The diffusion measurements employ four spaced ring resonators. (B) the diffusion measurements employ four sets of three cascaded ring resonators where sodium chloride (salt) diffusion was measured (courtesy of IMEC [47]).

large volume applications such as medical diagnostics with disposable and low-cost cartridges [47].

In order to provide solutions to all these challenges, there are efforts such as the PIX4life project [69]. This initiative focuses on developing a pilot line to support the development of visible and short NIR PICs at some of the most relevant wavelength ranges for bio- and life science: 405 nm, 455 nm, 530–562 nm, 625–660 nm, and 785–850 nm. In order to reduce the cost of design and fabrication of new PICs, several basic building blocks are being designed, fabricated, characterized, and validated, at those wavelength ranges, and they are starting to be offered at different PDKs [60, 61] for two different foundries [78, 79].

6 Conclusion

In this tutorial we have briefly discussed the current technology platforms to develop PICs, with a short review of devices and systems implemented in both SiN and PLC. The basic building blocks currently reported for visible PICs have been described. These compose the PDKs provided by the open-access foundries, fundamental for the reliable and repeatable fabrication of a photonic circuit. Along with the PDKs, a designer can employ different tools, which model and simulate building blocks and circuits, to implement the required system functionality. The circuit design is then ready for layout into a mask and checked via the specific DRC for each foundry. Characterization and packaging will be required, and they need to be accounted for in the early development stages.

We have also briefly described the challenges this technology has yet to overcome. However, as can be observed from the referred publications, several research groups, companies, and consortia are pushing the boundaries toward maturing the design frameworks, manufacturing platforms and packaging, and test solutions.

Acknowledgment: This work was supported by the European Union's Horizon 2020 research and innovations program, under the grant agreement no. 688519 (PIX4life).

References

[1] K. Yamada, J. Liu, T. Baba, L. Vivien, D.-X. Xu, et al., Photonic Integration and Photonics-Electronics Convergence on Silicon Platform (Frontiers Media SA, Lausanne, Switzerland, 2015).

[2] R. Soref, IEEE J. Sel. Top. Quantum Electron. 12, 1678–1687 (2006).

[3] A. E.-J. Lim, J. Song, F. Qing, C. Li, X. Tu, et al., IEEE J. Sel. Top. Quantum Electron. 20, 405–416 (2014).

[4] P. Muñoz, G. Mico, L. A. Bru, D. Pastor, D. Pérez, et al., Sensors 17, 2088 (2017).

[5] R. G. Heideman, R. P. H. Kooyman, and J. Greve, Sens. Actuat. B: Chem. 10, 209–217 (1993).

[6] E. F. Schipper, A. M. Brugman, L. M. Lechuga, L. M. Lechuga, R. P. H. Kooyman, et al., Sens. Actuat. B: Chem. 40, 147–153 (1997).

[7] A. Fernández Gavela, D. Grajales Garca, J. C. Ramirez, and L. M. Lechuga, Sensors 16, 285 (2016).

[8] W. Bogaerts, R. Baets, P. Dumon, V. Wiaux, S. Beckx, et al., J. Lightwave Technol. 23, 401–412 (2005).

[9] R. Heideman, A. Leinse, W. Hoving, R. Dekker, D. H. Geuzebroek, et al., Proc. SPIE 7221, 7221-7221-15 (2009). doi: 10.1117/12.808409.

[10] C. Monat, P. Domachuk and B. J. Eggleton, Nat. Photonics 1, 106–114 (2007).

[11] M. J. Shaw, J. Guo, G. A. Vawter, S. Habermehl and C. T. Sullivan, MOEMS 5720 (2005), 109–118.

[12] A. Yalcin, K. C. Popat, J. C. Aldridge, T. A. Desai, J. Hryniewicz, et al., IEEE J. Sel. Top. Quantum Electron. 12, 148–155 (2006).

[13] A. Schimpf, F. Canto, D. Bucci, A. Magnaldo, L. Couston, et al., In: '2011 2nd International Conference on Microfluidics and Integrated Optics Glass Sensor for In-line Microprobing of Nuclear Samples in Advancements in Nuclear Instrumentation Measurement Methods and Their Applications (ANIMMA) (IEEE, 2011), 1–7.

[14] I. D. Block, L. L. Chan and B. T. Cunningham, Sens. Actuat. B: Chem. 120, 187–193 (2006).

[15] A. H. Hosseinnia, A. H. Atabaki, A. A. Eftekhar and A. Adibi, Opt. Express 23, 30297 (2015).

[16] G. A. J. Besselink, R. G. Heideman, E. Schreuder, L. S. Wevers, F. Falke, et al. Biosens. Bioelectron. 7, 1–11 (2016).

[17] D. McCloskey and J. F. Donegan, Silicon nitride microdisks in the visible range in Transparent Optical Networks (ICTON), 2011 13th International Conference on (IEEE, 2011), 1–4.

[18] D. N. Urrios, F. F. Lupi, J. Montserrat, C. Domínguez, P. Pellegrino, et al., Optical characterisation of high Q silicon rich silicon nitride u-disks in the visible range in CLEO/Europe and EQEC 2011 Conference Digest (2011), paper CK2_4 The European Conference on Lasers and Electro-Optics (Optical Society of America, 2011), CK2_4.

[19] S. Romero-Garca, F. Merget, F. Zhong, H. Finkelstein and J. Witzens, Opt. Lett. 38, 2521–2523 (2013).

[20] S. Romero-Garcia, T. Klos, E. Klein, J. Leuermann, D. Geuzebroek, et al., Proc. SPIE, 101080 (2017).

[21] D. Martens, A. Z. Subramanian, S. Pathak, M. Vanslembrouck, P. Bienstman, et al., IEEE Photon. Technol. Lett. 27, 137–140 (2015).

[22] D. Geuzebroek, A. van Rees, E. Klein and K. Lawniczuk, Visible arrayed waveguide grating (400 nm–700 nm) for ultra-wide band (400–1700 nm) integrated spectrometer for spectral tissue sensing. in CLEO/Europe and EQEC 2017 Conference Digest (2017).

[23] G. Calafiore, A. Koshelev, S. Dhuey, A. Goltsov, P. Sasorov, et al., Light Sci. Appl. 3, e203 (2014).

[24] X. Nie, E. Ryckeboer, G. Roelkens and R. Baets, Opt. Express 25, A409 (2017).

[25] C. H. Henry, R. F. Kazarinov, H. J. Lee, K. J. Orlowsky and L. E. Katz LE, Appl. Opt. 26, 2621 (1987).

[26] J. F. Bauters, M. J. Heck, D. John, D. Dai, M. C. Tien, et al., Opt. Express 19, 3163–3174 (2011).

[27] A. Leinse, R. G. Heideman, E. J. Klein, R. Dekker, C. G. H. Roeloffzen, et al., TriPleX™ platform technology for photonic integration: applications from UV through NIR to IR in Information Photonics (IP), 2011 ICO International Conference on (IEEE, 2011), 1–2.

[28] S. Romero-García, F. Merget, F. Zhong, H. Finkelstein and J. Witzens, Opt. Express 21, 14036 (2013).

[29] A. Z. Subramanian, P. Neutens, A. Dhakal, R. Jansen, T. Claes, et al., IEEE Photon. J. 5, 2202809 (2013).

[30] K. Misiakos, I. Raptis, A. Salapatas, E. Makarona, A. Botsialas, et al., Opt. Express 22, 8856 (2014).

[31] D. Duval, J. Osmond, S. Dante, C. Domínguez and L. M. Lechuga, IEEE Photon. J. 5, 3700108–3700108 (2013).

[32] F. Ghasemi, A. A. Eftekhar, D. S. Gottfried, X. Song, R. D. Cummings, et al., Self-referenced silicon nitride array microring biosensor for toxin detection using glycans at visible wavelength in (2013), 85940A.

[33] C. A. Barrios, Anal. Bioanal. Chem. 403, 1467–1475 (2012).

[34] L. Martiradonna, F. Pisanello, T. Stomeo, A. Qualtieri, G. Vecchio, et al., Silicon nitride photonic crystal nanocavities for biochip applications in Transparent Optical Networks (ICTON), 2011 13th International Conference on (IEEE, 2011), 1–4.

[35] P. V. Lambeck, Integrated optical sensors for the chemical domain. Meas. Sci. Technol. 17, R93–R116 (2006).

[36] F. Prieto, B. Sepúlveda, A. Calle, A. Llobera, C. Domínguez, et al., Nanotechnology 14, 907–912 (2003).

[37] F. Ghasemi, A. A. Eftekhar, H. S. Mousavi, R. Abbaspour, H. Moradinejad, et al., Lab-on-chip Silicon Nitride Microring Sensor at Visible Wavelength Using Glycoprotein Receptors in CLEO: Applications and Technology (Optical Society of America, 2014), AW1L–3.

[38] J. Maldonado, A. B. González-Guerrero, C. Domínguez and L. M. Lechuga, Biosens. Bioelectron. 85, 310–316 (2016).

[39] M. Welkenhuysen, L. Hoffman, Z. Luo, A. De Proft, C. Van den Haute, et al., Sci. Rep. 6, 1–10 (2016).

[40] J. P. Epping, T. Hellwig, M. Hoekman, R. Mateman, A. Leinse, et al., Opt. Express 23, 19596–19604 (2015).

[41] M. A. G. Porcel, F. Schepers, J. P. Epping, T. Hellwig and M. Hoekman, et al., Opt. Express 25, 1542 (2017).

[42] D. J. Moss, R. Morandotti, A. L. Gaeta and M. Lipson, Nat. Photonics 7, 597–607 (2013).

[43] S. Sabouri, M. Namdari, S. Hosseini and K. Jamshidi, 1-D array of silicon nitride grating couplers for visible light communications in Wireless for Space and Extreme Environments (WiSEE), 2016 IEEE International Conference on (IEEE, 2016), 73–76.

[44] M. Raval, A. Yaacobi, D. Coleman, N. M. Fahrenkopf, C. Baiocco, et al., Nanophotonic phased array for visible light image projection in Photonics Conference (IPC) (IEEE, 2016), 206–207.

[45] M. J. Heck, Nanophotonics 6, 93–107 (2016).

[46] P. Muellner, E. Melnika, G. Koppitsch, J. Kraft, F. Schrank, et al., Procedia Eng. 120, 578–581 (2015).

[47] E. Ryckeboer, J. Vierendeels, A. Lee, S. Werquin, P. Bienstman, et al., Lab Chip 13, 4392 (2013).
[48] D. Bischof, F. Kehl and M. Michler, Opt. Commun. 380, 273–279 (2016).
[49] X.-J. Liu, J.-J. Zhang, X.-W. Sun, Y.-B. Pan, L.-P. Huang, et al., Thin Solid Films 460, 72–77 (2004).
[50] R. G. Heideman, A. Melloni, M. Hoekman, A. Borreman, A. Leinse, et al., Proc. IEEE Benelux, 71–74 (2005).
[51] A. Z. Subramanian, E. Ryckeboer, A. Dhakal, F. Peyskens, A. Malik, et al., Photon. Res. 3, 47–59 (2015).
[52] T. Chalyan, L. Pasquardini, F. Falke, M. Zanetti, R. Guider, et al., Proc. SPIE 9899, 1–9 (2016).
[53] B. Sepúlveda, J. Sánchez del Río, M. Moreno, F. J. Blanco, K. Mayora, et al., J. Opt. A Pure Appl. Opt. 8, S561–S566 (2006).
[54] T. Claes, W. Bogaerts and P. Bienstman, Opt. Lett. 36, 3320 (2011).
[55] D. Dai, Z. Wang, J. F. Bauters, M.-C. Tien, M. J. R. Heck, et al., Opt. Express 19, 14130–14136 (2011).
[56] K. Zinoviev, L. G. Carrascosa, J. Sánchez del Río, B. Sepúlveda, C. Domínguez, et al., Adv. Opt. Technol. 2008, 1–6 (2008).
[57] F. Ghasemi, M. Chamanzar, E. S. Hosseini, A. A. Eftekhar, Q. Li, et al., Compact fluorescence sensor using on-chip silicon nitride microdisk in Photonics Conference (PHO) (IEEE, 2011), 151–152.
[58] M. Mahmud-Ul-Hasan, P. Neutens, R. Vos, L. Lagae, P. V. Dorpe, et al., ACS Photonics 4, 495–500 (2017).
[59] T. Korthorst, R. Stoffer and A. Bakker, Adv. Opt. Technol. 4, 147–155 (2015).
[60] Luceda. http://www.lucedaphotonics.com/.
[61] PhoeniX Software – Solutions for micro and nano technologies. http://www.phoenixbv.com/.
[62] Photon Design. https://www.photond.com/.
[63] RSoft Products. https://www.synopsys.com/optical-solutions/rsoft.html.
[64] Optiwave. https://optiwave.com/.
[65] Lumerical Inc. / Innovative Photonic Design Tools
[66] COMSOL Wave Optics Simulation Software. https://www.comsol.com/wave-optics-module.
[67] L. Bolla, ElectroMagnetic-Python version 0.1.2.
[68] Prototyping multi project wafer runs. www.europracticeic.com.
[69] PIX4life. http://www.pix4life.eu/.
[70] PIXAPP. http://www.pixapp.eu/.
[71] T. Claes, W. Bogaerts and P. Bienstman, Opt. Express 18, 22747 (2010).
[72] R. Dekker, E. Klein and D. Geuzebroek, Polarization maintaining single mode color combining using TriPleX™ based integrated optics for biophotonic applications in (IEEE, 2012), 286–287.
[73] L. Chang, M. H. P. Pfeiffer, N. Volet, M. Zervas, J. D. Peters, et al., Opt. Lett. 42, 803–806 (2017).
[74] M. J. R. Heck, J. F. Bauters, M. L. Davenport, K. K. Doylend, S. Jain, et al., IEEE J. Sel. Top. Quantum Electron. 19, 6100117–6100117 (2013).
[75] E. P. Haglund, S. Kumari, E. Haglund, J. Gustavsson, R. G. Baets, et al., IEEE J. Sel. Top. Quantum Electron. 23, 1–9 (2017).
[76] D. K. Schroder, Semiconductor Material and Device Characterization (Wiley, Hoboken, NJ, USA, 1998).
[77] S. Kumari, E. P. Haglund, J. S. Gustavsson, A. Larsson, G. Roelkens, et al., Design of an intra-cavity SiN grating for integrated 850nm VCSELs in Proceedings Symposium IEEE Photonics Society Benelux (2016), 263–266.
[78] LioniX International. http://www.lionix-international.com/.
[79] Imec R&D, nano electronics and digital technologies. https://www.imec-int.com/.

Marco A.G. Porcel
VLC Photonics, Ed. 9B, D2, UPV, Camino de vera sn, 46022 Valencia, Spain
marco.garcia@vlcphotonics.com

Marco A.G. Porcel obtained his MSc in Telecom Engineering at the Polytechnic University of Valencia (UPV, Spain) in 2011. He continued with his PhD degree (defended on December 2017) on nonlinear control of light in integrated waveguides at the Laser Physics and Nonlinear Optics group (LPNO) part of the MESA+ Institute for Nanotechnology at the University of Twente (The Netherlands). In 2017, he joined VLC Photonics as the R&D Manager, working on the field of photonic integrated circuits.

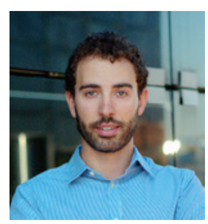

Iñigo Artundo
VLC Photonics, Ed. 9B, D2, UPV, Camino de vera sn, 46022 Valencia, Spain

Iñigo Artundo obtained his MSc in Telecom Engineering at the Universidad Publica de Navarra (Pamplona, Spain) in 2005 and received his PhD in Applied Physics and Photonics at the Vrije Universiteit Brussel (Brussels, Belgium) in 2009. He has been involved in several national and European research projects and networks of excellence focused on optical telecom and interconnects, micro-optics, and photonic integration. He has worked as a reviewer for several scientific journals, national and international funding agencies. He holds specializations in Business Financing, Commercial Management and Research, and Strategic Marketing. He is a member of IEEE, SPIE, and COIT. He currently is the CEO of VLC Photonics, working in the field of photonic integrated circuits.

J. David Domenech
VLC Photonics, Ed. 9B, D2, UPV, Camino de vera sn, 46022 Valencia, Spain

J. David Domenech received his BSc degree in Telecommunications and his MSc degree in Technologies, Systems and Networks of Communication from the Universidad Politecnica de Valencia (UPV) in 2006 and 2008, respectively. He obtained his PhD degree in Optics at the Telecommunications and Multimedia Applications Institute (iTEAM) from UPV, inside the Optical and Quantum Communications Group, focusing his research in the use of integrated ring resonators for microwave photonics applications. Since 2006, he has been working on the design of integrated optic circuits in indium phosphide/silicon nitride/SOI technologies within several European and national research projects. In 2012, he was awarded with the Intel PhD Honor Programme award. He is currently the CTO of VLC Photonics, working in the field of photonic integrated circuits.

Douwe Geuzebroek
LioniX International, Hengelosestraat 500
7521 AN Enschede, The Netherlands

Douwe Geuzebroek is the VP of sales and marketing at LioniX International. He holds a masters degree in Electrical Engineering of the University of Twente and did a PhD research at the Integrated Optical MicroSystems group on the topic of ‘Flexible Optical Network Components Based on Densely Integrated Micro-ring Resonators’. Besides this, he finished an introduction program at the TSM Business School. In 2005, he joined LioniX b.v. as a design engineer and project leader focusing on micro-ring resonators and other integrated optical telecommunication devices and was actively involved in the start-up of XiO Photonics in 2009.

Rino Sunarto
PhoeniX Software B. V., Capitool 50, 7521 PL
Enschede, The Netherlands

Rino Sunarto studied at the Saint Joseph College Malang and obtained his BEng on Electrical and Electronic Engineering in 2008 at the Saxion University of Applied Sciences. He was an ASIC design engineer at Bruco B. V. from 2008 to 2009, a junior design engineer at XiO Photonics from 2009 to 2011, and now works as a software engineer at PhoeniX Software.

Romano Hoofman
IMEC, Kapeldreef 75, 3001 Heverlee, Belgium

Romano Hoofman received his MSc degree in Molecular Sciences from Wageningen University in the Netherlands in 1995 and his PhD degree in Radiation Chemistry from the Technological University of Delft, The Netherlands, in 2000. He started his career in the industry where he worked as a principal scientist at Philips Research and later on at NXP Semiconductors. He covered many different R&D topics, ranging from CMOS integration, photovoltaic technology, thin-film batteries, and sensors (which form together the building blocks for IoT sensor nodes). Currently, he is a program director at IMEC, where he is responsible for the project management of Europractice and related services.